Ultrafast Spin Dynamics Including Spin-Orbit Interaction in Semiconductors

Michael Krauß,* Martin Aeschlimann, and Hans Christian Schneider†
Physics Department and Research Center OPTIMAS, University of Kaiserslautern, P.O. Box 3049, 67663 Kaiserslautern, Germany
(Received 2 January 2008; published 26 June 2008)

This Letter presents a theoretical investigation of ultrafast spin-dependent carrier dynamics in semiconductors due to strong spin-orbit coupling using holes in bulk GaAs as a model system. By computing the microscopic carrier dynamics in the anisotropic hole-band structure including spin-orbit coupling, we obtain spin-relaxation times in quantitative agreement with measured hole-spin relaxation times [Phys. Rev. Lett. **89**, 146601 (2002)]. We show that different optical techniques for the measurement of hole-spin dynamics yield different results, in contrast to the case of electron-spin dynamics.

DOI: 10.1103/PhysRevLett.100.256601 PACS numbers: 72.25.Rb, 71.70.Ej, 72.25.Fe, 78.47.−p

Research on spin-dependent carrier dynamics in semiconductors is progressing in different directions [1–4]. Although there is a push towards the physics of spintronics devices where long-lived electron-spin polarizations and their transport properties over macroscopic distances are of particular interest, there are still important questions regarding the microscopic details of the complex carrier spin dynamics in semiconductors. For instance, ultrafast spin-dependent dynamics on picosecond or subpicosecond time scales have become accessible using different experimental techniques in recent years, which show that a detailed microscopic understanding of the processes contributing to spin relaxation on these time scales is impossible using simplified relaxation-time approximations [5–7]. For several reasons, such a microscopic understanding is valuable not only for electrons but also for holes. First, holes play an important role for magnetic correlations in diluted magnetic semiconductors [8], and the hole spin may be used as a carrier of information [9]. Second, from a fundamental point of view, holes in III–V semiconductors are a model system for spin relaxation with pronounced spin-orbit (SO) coupling. The SO coupling leads to a strong momentum-dependent mixing of spin and orbital-momentum eigenstates, so that scattering processes change spin and orbital angular momentum [10–12]. Although both electrons and holes are affected by this relaxation mechanism, it causes a much faster spin relaxation for the p-like holes than the s-like electrons, because the former experience the SO coupling directly, while the latter are only coupled to remote bands with a finite orbital momentum.

In this Letter, we compute the ultrafast microscopic hole dynamics and relate it to experimentally accessible quantities. We determine the quasiparticle states in the presence of the SO interaction from a $k \cdot p$ calculation, and use them as input for the calculation of the microscopic, i.e., momentum and time dependent, carrier distribution functions including the relevant interaction mechanisms in bulk GaAs. Thus our approach differs, on the one hand, from recent work that concentrates on the band-structure calculation, but replaces the complicated dynamics with the assumption of an energy-dependent exponential decay of a quasiequilibrium spin polarization [13–15]. On the other hand, we treat the influence of the anisotropic quasiparticle states in bulk GaAs due to the SO interaction, which has not been included in existing microscopic approaches to the spin-dependent carrier scattering dynamics [16,17]. By combining a sufficiently realistic band structure with a microscopic calculation of the carrier dynamics, we achieve (i) a quantitative physical picture of the complex hole-spin dynamics, and (ii) an accurate determination of physical quantities accessible by time-resolved 2-photon photoemission [18], Faraday effect [19], and differential transmission experiments [20].

The electron and hole states around the fundamental band gap are calculated at the level of an eight-band Kane model, i.e., a $k \cdot p$ Hamiltonian $\mathcal{H}(\vec{k})$ with 6 hole and 2 electron bands containing terms up to second order in k [21]. Diagonalization of $\mathcal{H}(\vec{k})$ yields the orthonormalized quasiparticle states $|\nu, \vec{k}\rangle$ and energy dispersions $\varepsilon_{\nu,\vec{k}}$, where the label $\nu = (b, p)$ includes the band index $b = E$, HH, LH, SOH, for electrons, heavy holes, light holes, and split-off holes, respectively, as well as the pseudospin $p = 1, 2$. The pseudospin can be introduced because the quasiparticle dispersions of all four types of carriers are (nearly) doubly degenerate. Note that the quasiparticle states include SO coupling, so that they constitute the "intelligent basis" in the sense of Ref. [22]. Using these single-quasiparticle states, a dynamical equation for the spin-density matrix including the scattering and dephasing contributions due to carrier-carrier and carrier-phonon interactions can be derived using a many-particle formalism, e.g., along the lines of Ref. [23]. In principle, one needs to track the time development of the coherences between different bands, which are related to the coherent spin precession, and the carrier distributions $n_{\nu,\vec{k}}$, which are related to the incoherent carrier dynamics [10]. These coherences between single-particle states can be driven by optical fields, but not by the SO interaction, because we work in the "intelligent basis." For the excitation conditions investigated in this Letter, we have checked numerically that the coherences driven by the fields are about 2 orders of magnitude smaller than the incoherent carrier distributions. This is because a polarized optical field predominantly creates heavy holes with momentum (anti)parallel to their spin orientation [24], which suppresses spin precession [9]. (See also the discussion of Fig. 1(a) below.) We therefore consider only the dynamics of the carrier distributions under the influence of carrier-carrier and carrier-phonon scattering [25]:

$$\frac{\partial}{\partial t} n_{\nu,\vec{k}} = \Gamma^{\rm in}_{\nu,\vec{k}}(1 - n_{\nu,\vec{k}}) - \Gamma^{\rm out}_{\nu,\vec{k}} n_{\nu,\vec{k}}. \quad (1)$$

The dynamical in-scattering rate consists of the carrier-carrier interaction contribution

$$\begin{aligned}\Gamma^{\rm in}_{\nu,\vec{k}}|_{\rm c\text{-}c} = \frac{2\pi}{\hbar} \sum_{\nu_1,\nu_2,\nu_3} \sum_{\vec{k}_1,\vec{q}} & n_{\nu_1,\vec{k}+\vec{q}}(1 - n_{\nu_2,\vec{k}_1+\vec{q}}) \\ & \times n_{\nu_3,\vec{k}_1} |\langle \nu_1, \vec{k} + \vec{q} | \nu, \vec{k}\rangle|^2 \\ & \times |\langle \nu_3, \vec{k}_1 | \nu_2, \vec{k}_1 + \vec{q}\rangle|^2 |v^s_q(\Delta\varepsilon)|^2 \\ & \times \delta(\varepsilon_{\nu,\vec{k}} - \varepsilon_{\nu_1,\vec{k}+\vec{q}} + \varepsilon_{\nu_2,\vec{k}_1+\vec{q}} - \varepsilon_{\nu_3,\vec{k}_1}) \quad (2)\end{aligned}$$

and a similar contribution due to the carrier-phonon interaction; see, e.g., Ref. [16], which includes room-temperature LO and LA phonons. The outscattering rate $\Gamma^{\rm out}$ is obtained from $\Gamma^{\rm in}$ by exchanging $(1 - n)$ with n. In Eq. (2), $\Delta\varepsilon = \varepsilon_{\nu,\vec{k}} - \varepsilon_{\nu_1,\vec{k}+\vec{q}}$, and $v^s_q(\Delta\varepsilon)$ is the 3D dynamically screened Coulomb potential, which is computed using the Lindhard dielectric function [26]. Equation (2) describes two-particle scattering processes connecting states $|\nu, \vec{k}\rangle \rightarrow |\nu_1, \vec{k} + \vec{q}\rangle$ and $|\nu_2, \vec{k}_1 + \vec{q}\rangle \rightarrow |\nu_3, \vec{k}_1\rangle$. Note that these scattering events change the admixture of spin from initial to final quasiparticle states [10,11], as can be seen from the nonvanishing overlaps $\langle \nu', \vec{k}' | \nu, \vec{k}\rangle$ in Eq. (2). This yields a nonequilibrium Elliott-Yafet-like spin dynamics for holes.

In order to compare our results with experimental approaches using optical orientation of carriers, we also take into account the optical excitation of a spin-polarized electron-hole plasma in the semiconductor for a σ_+-polarized ultrashort pulse traveling in the z, or (001), direction. The excitation process is modeled by an initial condition for the carrier distributions $n_{\nu,\vec{k}}(t = 0) = \sum_\mu |\vec{d}_{\mu\nu}(\vec{k}) \cdot \vec{E}|^2 g(\hbar\omega - \varepsilon_{\mu,\vec{k}} - \varepsilon_{\nu,\vec{k}})$ with the dipole-matrix elements $\vec{d}_{\mu\nu}(\vec{k}) = e\langle \mu, \vec{k} | \vec{r} | \nu, \vec{k}\rangle$, the amplitude $\vec{E}$ and photon energy $\hbar\omega$ of the exciting field, and a Gaussian broadening function g peaked at $\hbar\omega - \varepsilon_{\mu,\vec{k}} - \varepsilon_{\nu,\vec{k}}$ [26]. The anisotropy of the carrier distributions is taken into account by an expansion of $n_{\nu,\vec{k}}(t)$ into spherical harmonics $Y_{\ell,m}(\hat{k})$ up to $\ell = 4$ where we retain only the expansion coefficients with radial or cubic symmetry, because these are the dominant symmetries of the Hamiltonian $\mathcal{H}$ [21].

As a typical excitation scenario we take an ultrashort 800 nm pulse (photon energy of $\hbar\omega = 1.55$ eV), which leads to a total carrier density of 1×10^{17} cm^{-3}. Figure 1(a) shows that these distributions are anisotropic, with hole momenta predominantly in the z ($\vartheta = 0$) and $-z$ ($\vartheta = \pi$) direction, due to the anisotropic dipole-matrix elements [24].

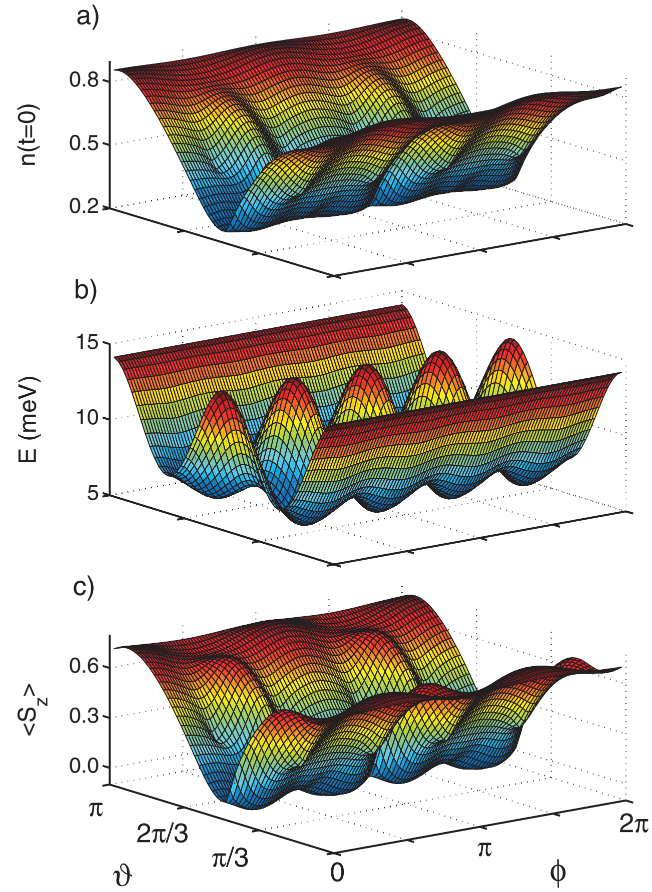

FIG. 1 (color). (a) Initial carrier distribution, (b) energy dispersion, and (c) average spin content $\langle S_z\rangle$ in the HH1 band as a function of quasiparticle-momentum direction. Here ϑ and ϕ are, respectively, the azimuthal and radial components of the hole momentum vector in polar coordinates. The plots are for $k = 0.4$ nm^{-1}, but the dependence on the modulus k is weak.

In the following, we distinguish between two polarizations: the spin polarization and the quasiparticle polarization. The latter is defined for electron, heavy hole, light hole, and split-off bands by

$$P^{(b)} = \frac{N_{b,1} - N_{b,2}}{N_{b,1} + N_{b,2}}. \quad (3)$$

In Eq. (3), $N_{b,p}$ denotes the number density for carriers in quasiparticle band $b = E$, HH, LH, or SOH, with pseudospin $p = 1$ and 2. Figure 2 shows the quasiparticle polarization, $P^{(b)}$, computed according to Eq. (3) for $b =$ HH and LH. The LH densities are appreciably changed due to interband scattering events, so that the LH quasiparticle polarization dynamics cannot be described by an exponential decay. This has also been noted for the experiment in

Ref. [20], where it was impossible to determine a relaxation time for the LH polarization by an exponential fit. As shown in the inset in Fig. 2, the number of carriers in the LH band decreases with equilibration (due to their smaller mass), so that the total polarization is dominated by the HH polarization, on which we will concentrate in the following [27].

To extract the dynamical spin polarization of the HH system from the quasiparticle distribution functions $n_{\nu,\vec{k}}(t)$, one calculates

$$\langle S_\alpha \rangle^{(\mathrm{HH})} = \frac{1}{N_{\mathrm{HH}}} \sum_{\vec{k}} \sum_{p=1,2} \langle \mathrm{HH}, p, \vec{k} | S_\alpha | \mathrm{HH}, p, \vec{k} \rangle n_{\mathrm{HH},p,\vec{k}}. \tag{4}$$

Here, $N_{\mathrm{HH}} = N_{\mathrm{HH},1} + N_{\mathrm{HH},2}$ is the density of HHs, and $\langle \nu, \vec{k} | S_\alpha | \nu, \vec{k} \rangle$, $\alpha = x, y, z$, is the "spin content" of a quasiparticle state $|\nu, \vec{k}\rangle$, as shown in Fig. 1(c). Figure 1(c) also shows that there are regions of $\vec{k}$ space with high average spin per particle, so-called spin "hot spots," which almost coincide with the maxima of the quasiparticle distribution created by the optical field shown in Fig. 1(a); i.e., the optical field creates the majority of quasiparticles in momentum states where the contribution to the spin polarization is high.

The computed dynamics of the quasiparticle polarization, Eq. (3), the spin polarization $\langle S_z \rangle^{(\mathrm{HH})}$, Eq. (4), and the differential transmission are shown in Fig. 3. Note that for the first 100 fs the nonequilibrium multiband scattering dynamics yields a nonexponential polarization decay, and that our calculation predicts that different techniques, such as 2-photon photoemission and differential transmission, will yield different spin-relaxation times. Also, the difference between the quasiparticle and spin polarizations is a generic feature of carrier dynamics with strong SO interaction. A qualitative picture of the different quasiparticle and spin dynamics can be obtained from Fig. 1. Quasiparticles in the hole bands are created by the optical field preferentially in the spin hot spots, but during the subsequent equilibration, quasiparticle scattering moves the carriers into the minima of the HH energy dispersion. As shown for the HH1 band in Fig. 1 these minima [in 1(b)] occur away from spin hot spots [maxima in 1(c)], so that the spin polarization can be lowered by all possible quasiparticle scattering events including those that change neither the band index nor the pseudospin. The quasiparticle polarization is affected only by transitions that change the band index b and/or the pseudospin p. The spin polarization therefore should decay faster than the quasiparticle polarization, and these qualitative considerations are validated by the full calculation. Despite the more complicated dynamics at short times, we apply a linear fit to the curves in Fig. 2 to obtain relaxation times of 180 fs and 140 fs for the quasiparticle and spin polarizations, respectively.

Figure 3 also shows the dynamics of the differential transmission calculated for the setup used in Ref. [20]. Using the dipole-matrix elements between the split-off and the HH bands from the eight-band Kane model, we determine the absorption of a 3.2 μm ultrashort probe pulse [28]. This yields a ratio between the absorption of σ_+- and σ_--polarized light shown in Fig. 3, which is usually interpreted as a measure of the spin polarization. The fit yields a value of around 125 fs, and thus a good agreement with the measurement of 110 fs in Ref. [20]. For smaller excitation photon energies, i.e., excitation of carriers closer to the band gap, our calculations predict only

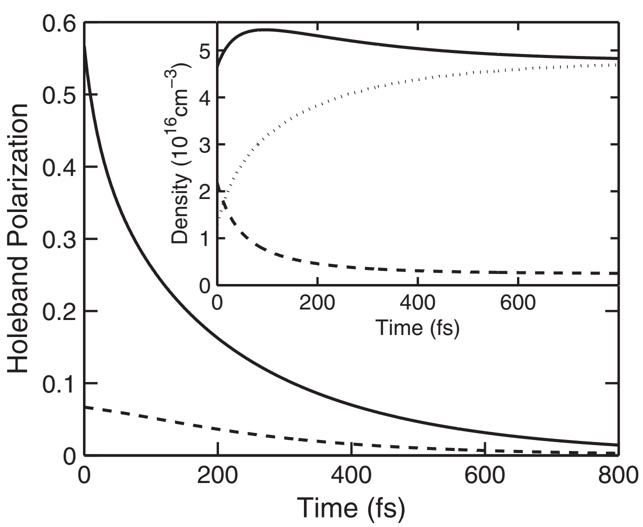

FIG. 2. Computed quasiparticle polarizations for HHs, $P^{(\mathrm{HH})}$ (solid line) and LHs, $P^{(\mathrm{LH})}$ (dashed line). Inset: Time dependence of the total density for HH1 (solid line), HH2 (dotted line), as well as LH1 (dashed line). The curves for LH1 and LH2 are indistinguishable in this plot.

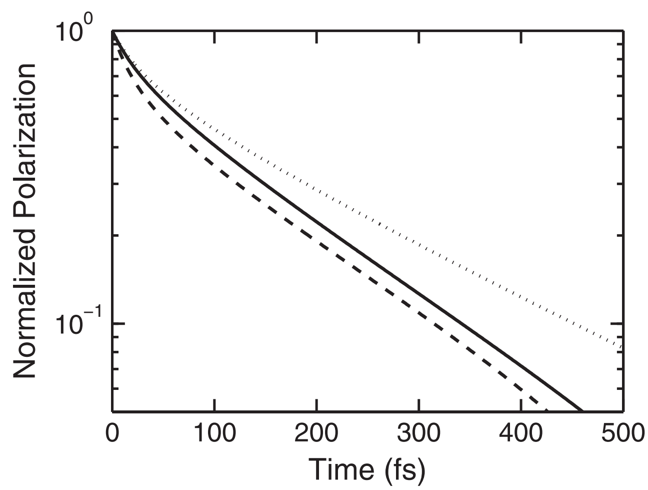

FIG. 3. Logarithmic plot of computed HH quasiparticle (dotted line) and spin (solid line) polarizations, as well as computed differential transmission for a 3.2 μm probe field (dashed line). Linear fits yield relaxation times of 180 fs, 140 fs, and 125 fs, respectively.

slightly larger relaxation times for the polarizations and the differential transmission.

Our numerical results and predictions should be compared to the theoretical investigations of hole-spin dynamics in Refs. [9,13]. In Ref. [13], an energy-independent spin-relaxation time of about 0.2 ps for heavy holes is calculated using the Elliott-Yafet relaxation rate. Although this result is on the same order of magnitude as the experiment and our theoretical result [20], this approach describes the spin dynamics of quasiequilibrium holes at low densities, and therefore cannot capture the pronounced nonequilibrium dynamics occurring over the first few hundred femtoseconds [7]. Reference [9] obtains a D'yakonov-Perel'-like picture of hole-spin relaxation due to spin precession described by a quadrupole term in the 4×4 Luttinger Hamiltonian. As discussed in connection with Fig. 1(a), this precessional dynamics is strongly suppressed for the case of polarized optical excitation.

In conclusion, we have investigated carrier-spin dynamics under the influence of strong SO coupling for the case of holes in bulk GaAs using a microscopic approach. Because of the strong SO coupling, we find a contribution to the spin dynamics from quasiparticle scattering out of spin hot spots. In particular, this leads to different relaxation times for the quasiparticle polarization, the spin polarization, and the polarization extracted from differential transmission measurements. This is in contrast to electron dynamics, where these quantities coincide and are used interchangeably as a measure of the spin polarization. Our calculation is in good agreement with experiments, but also shows that a careful analysis of the experimental setup is necessary to achieve this agreement.

We thank M.-W. Wu and M. Fleischhauer for helpful discussions, and the Bosch Stiftung for support. A grant for CPU time from the NIC Jülich is gratefully acknowledged.

*mkrauss@physik.uni-kl.de
†hcsch@physik.uni-kl.de

[1] *Semiconductor Spintronics and Quantum Computation*, edited by D. D. Awschalom, D. Loss, and N. Samarth (Springer, Berlin, 2002).
[2] S. A. Wolf, D. D. Awschalom, R. A. Buhrman, J. M. Daughton, S. von Molnar, M. L. Roukes, A. Y. Chtchelkanova, and D. M. Treger, Science **294**, 1488 (2001).
[3] I. Žutić, J. Fabian, and S. Das Sarma, Rev. Mod. Phys. **76**, 323 (2004).
[4] J. S. Sandhu, A. P. Heberle, J. J. Baumberg, and J. R. A. Cleaver, Phys. Rev. Lett. **86**, 2150 (2001).
[5] M. M. Glazov and E. L. Ivchenko, JETP Lett. **75**, 403 (2002).
[6] M. Q. Weng and M. W. Wu, Phys. Rev. B **68**, 075312 (2003).
[7] H. C. Schneider *et al.*, Phys. Rev. B **73**, 081302(R) (2006).
[8] T. Jungwirth, J. Sinova, J. Mašek, J. Kučera, and A. H. MacDonald, Rev. Mod. Phys. **78**, 809 (2006).
[9] D. Culcer, C. Lechner, and R. Winkler, Phys. Rev. Lett. **97**, 106601 (2006).
[10] L. J. Sham, J. Phys. Condens. Matter **5**, A51 (1993).
[11] N. S. Averkiev, L. E. Golub, and M. Willander, J. Phys. Condens. Matter **14**, R271 (2002).
[12] G. E. Pikus and A. N. Titkov, in *Optical Orientation*, edited by F. Meier and B. P. Zakharchenya (North-Holland, Amsterdam, 1984), pp. 73–131.
[13] Z. G. Yu, S. Krishnamurthy, M. van Schilfgaarde, and N. Newman, Phys. Rev. B **71**, 245312 (2005).
[14] A. Dyson and B. K. Ridley, Phys. Rev. B **69**, 125211 (2004).
[15] W. H. Lau, J. T. Olesberg, and M. E. Flatté, Phys. Rev. B **64**, 161301(R) (2001).
[16] C. Lu, J. L. Cheng, and M. W. Wu, Phys. Rev. B **73**, 125314 (2006).
[17] M. W. Wu and C. Z. Ning, Phys. Status Solidi B **222**, 523 (2000).
[18] M. Aeschlimann *et al.*, Phys. Rev. Lett. **79**, 5158 (1997).
[19] S. A. Crooker, D. D. Awschalom, J. J. Baumberg, F. Flack, and N. Samarth, Phys. Rev. B **56**, 7574 (1997).
[20] D. J. Hilton and C. L. Tang, Phys. Rev. Lett. **89**, 146601 (2002).
[21] R. Winkler, *Spin-Orbit Coupling Effects in Two-Dimensional Electron and Hole Systems* (Springer, Berlin, 2003).
[22] J. Fabian, A. Matos-Abiague, C. Ertler, P. Stano, and I. Žutić, Acta Phys. Slovaca **57**, 565 (2007).
[23] R. Binder and S. W. Koch, Prog. Quantum Electron. **19**, 307 (1995).
[24] V. D. Dymnikov, M. I. D'yakonov, and V. I. Perel', Sov. Phys. JETP **71**, 2373 (1976).
[25] J. H. Collet, Phys. Rev. B **47**, 10279 (1993).
[26] H. Haug and S. W. Koch, *Quantum Theory of the Optical and Electronic Properties of Semiconductors* (World Scientific, Singapore, 2004), 4th ed.
[27] The split-off hole bands are not populated under the excitation conditions assumed in this Letter.
[28] For details, especially the choice of the probe wavelength for the interpretation of the differential transmission measurements, see Ref. [20].